11106 *Inorg. Chem.* **2010**, *49*, 11106–11117
DOI: 10.1021/ic1016998

Inorganic Chemistry
Article

Iron(II) Complexes with Tetradentate Bis(aminophenolate) Ligands: Synthesis and Characterization, Solution Behavior, and Reactivity with O_2

Christopher J. Whiteoak, Rafael Torres Martin de Rosales, Andrew J. P. White, and George J. P. Britovsek*

Department of Chemistry, Imperial College London, Exhibition Road, London, SW7 2AY, United Kingdom

Received August 20, 2010

Tetradentate bis(aminophenolate) ligands H_2salan^X and H_2bapen^X (where X refers to the *para*-phenolate substituent = H, Me, F, Cl) react with $[Fe\{N(SiMe_3)_2\}_2]$ to form iron(II) complexes, which in the presence of suitable donor ligands L (L = pyridine or THF) can be isolated as the complexes $[Fe(salan^X)(L)_2]$ and $[Fe(bapen^X)(L)_2]$. In the absence of donor ligands, either mononuclear complexes, for example, $[Fe(salan^{tBu,tBu})]$, or dinuclear complexes of the type $[Fe(salan^X)]_2$ are obtained. The dynamic coordination behavior in solution of the complexes $[Fe(salan^F)(L)_2]$ and $[Fe(bapen^F)(L)_2]$ has been investigated by VT ^1H and ^{19}F NMR spectroscopy, which has revealed equilibria between isomers with different ligand coordination topologies cis-α, cis-β and trans. Exposure of the iron(II) $salan^X$ complexes to O_2 results in the formation of oxo-bridged iron(III) complexes of the type $[\{Fe(salan^X)\}_2(\mu\text{-}O)]$ or $[\{Fe(salan^X)(L)\}_2(\mu\text{-}O)]$. The lack of catalytic activity of the iron(II) salan and bapen complexes in the oxidation of cyclohexane with H_2O_2 as the oxidant is attributed to the rapid formation of stable and catalytically inactive oxo-bridged iron(III) complexes.

Introduction

Salen ligands are an important class of ligands due their versatility in terms of steric and electronic modifications, and many salen metal complexes have found important applications in homogeneous catalysis.[1] Well known examples are the manganese salen complexes used as alkene epoxidation catalysts[2] and the chromium and aluminum salen complexes applied in the ring-opening polymerization of epoxides with CO_2.[3,4] Iron-based salen complexes have been used in oxidation catalysis, for example, as mimics for the active site in oxygenases,[5−7] as catalysts for the oxidation of alkenes and alkanes with dioxygen[5,8−10] and for the oxidation of organic sulfides with strong oxidants such as PhIO.[11,12]

The related ligand class of salan ligands, also referred to as reduced salen or tetrahydrosalen ligands, has received comparatively less attention, probably because their synthesis is less straightforward. However, potential benefits, such as increased ligand flexibility and stronger nitrogen donors make them attractive ligand targets.[13] Some early studies on the synthesis and the characterization of iron complexes containing salan ligands were reported in the early 1980s by Borer and co-workers.[14,15] A dinuclear hydroxo-bridged iron(III) complex of class **A** $[Fe(salan)(\mu{-}OH)]_2$ was obtained by reacting the ligand with iron(II) salts in an aqueous environment (see Figure 1). The oxidation of Fe(II) to Fe(III) was probably caused by dioxygen from the air.[14] Similar dinuclear iron(III) methoxy-bridged complexes were later reported by others.[16−18] A different iron(III) salan complex was reported starting from $FeCl_3$ and H_2salan. On the basis of Mössbauer data, a dinuclear phenoxide-bridged structure $[Fe(\mu\text{-O-salan})Cl]_2$

*Corresponding author. E-mail: g.britovsek@imperial.ac.uk. Telephone: +44-(0)20-75945863.

(1) Cozzi, P. G. *Chem. Soc. Rev.* **2004**, *33*, 410–421.
(2) McGarrigle, E. M.; Gilheany, D. G. *Chem. Rev.* **2005**, *105*, 1563–1602.
(3) Darensbourg, D. J. *Chem. Rev.* **2007**, *107*, 2388–2410.
(4) Coates, G. W.; Moore, D. R. *Angew. Chem., Int. Ed.* **2004**, *43*, 6618–6639.
(5) Fujii, H.; Funahashi, Y. *Angew. Chem. Int. Ed.*. **2002**, *41*, 3638–3641.
(6) Kurahashi, T.; Oda, K.; Sugimoto, M.; Ogura, T.; Fujii, H. *Inorg. Chem.* **2006**, *45*, 7709–7721.
(7) Snyder, B. S.; Patterson, G. S.; Abrahamson, A. J.; Holm, R. H. *J. Am. Chem. Soc.* **1989**, *111*, 5214–5223.
(8) Böttcher, A.; Birnbaum, E. R.; Day, M. W.; Gray, H. B.; Grinstaff, M. W.; Labinger, J. A. *J. Mol. Catal. A: Chem.* **1997**, *117*, 229–242.
(9) Böttcher, A.; Grinstaff, M. W.; Labinger, J. A.; Gray, H. B. *J. Mol. Catal. A: Chem.* **1996**, *113*, 191–200.
(10) Tabushi, I.; Nakajima, T.; Seto, K. *Tetrahedron Lett.* **1980**, *21*, 2565–2568.
(11) Bryliakov, K. P.; Talsi, E. P. *Angew. Chem., Int. Ed.* **2004**, *43*, 5228–5230.
(12) Sivasubramanian, V. K.; Ganesan, M.; Rajagopal, S.; Ramaraj, R. *J. Org. Chem.* **2002**, *67*, 1506–1514.
(13) Matsumoto, K.; Saito, B.; Katsuki, T. *Chem. Commun.* **2007**, 3619–3627.
(14) Borer, L.; Thalken, L.; Ceccarelli, C.; Glick, M.; Zhang, J. H.; Reiff, W. M. *Inorg. Chem.* **1983**, *22*, 1719–1724.
(15) Borer, L.; Thalken, L.; Zhang, J. H.; Reiff, W. M. *Inorg. Chem.* **1983**, *22*, 3174–3176.
(16) Baran, P.; Böttcher, A.; Elias, H.; Haase, W.; Hüber, M.; Fuess, H.; Paulus, H. *Z. Naturforsch.* **1992**, *47B*, 1681–1686.
(17) Atwood, D. A.; Jegier, J. A.; Lindholm, N. F.; Martin, K. J.; Rutherford, D. *J. Coord. Chem.* **1996**, *38*, 305–318.
(18) Viswanathan, R.; Palaniandavar, M.; Prabakaran, P.; Muthiah, P. T. *Inorg. Chem.* **1998**, *37*, 3881.

Published on Web 11/09/2010

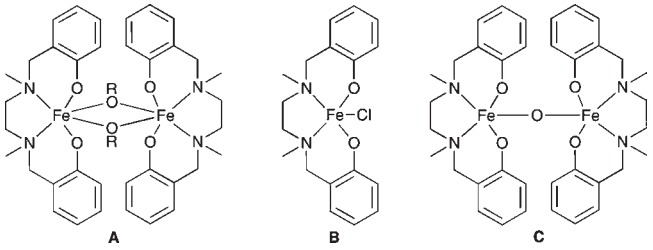

Figure 1. Examples of previously reported iron(III) salan complexes.

was proposed for this complex in the solid state.[15] More recently, the use of bulky substituents in the ortho position of the phenoxy moieties has allowed the isolation of several mononuclear complexes [Fe(salan)Cl] of class **B**.[19−22] A third class **C** comprises oxo-bridged dinuclear iron(III) salan complexes.[23] Oxo-bridged dinuclear iron(III) complexes [LFe−O−FeL] are plentiful and have long been known,[24] and their involvement in many nonheme enzymes and proteins is well established.[25]

All previously reported iron salan complexes have in common that the iron center is formally in the +3 oxidation state. To the best of our knowledge, no reports on iron(II) complexes containing salan ligands have been published so far. In contrast, iron(II) salen complexes have been known for some time.[26] It should be noted that iron(II) salen complexes [Fe(salen)], which are typically brown in color, are extremely air sensitive, as reported by Larkworthy and Calderazzo already in the late 1960s and more recently also by Do and Lippard.[27−29] In several reports where iron(II) salen complexes were believed to be obtained as orange/red, blue, or purple materials,[30−33] oxidation of iron(II) to iron(III) has probably taken place, most likely to give dinuclear oxo-bridged iron(III) complexes.

Here we present the synthesis and the characterization of the first iron(II) and ruthenium(II) salan complexes. A series of salan ligands and their corresponding iron(II) complexes has been prepared containing different substituents in the ortho- and para-position of the phenoxy donors (see Figure 2). Furthermore, we have prepared a series of novel iron(II)

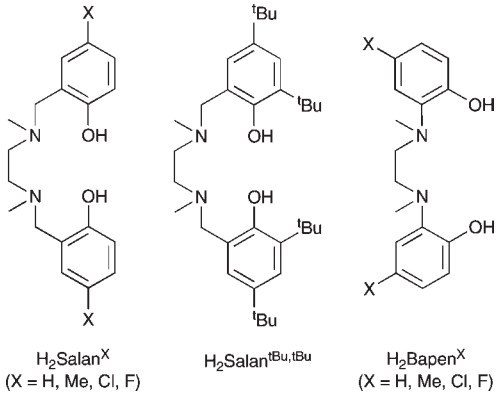

Figure 2. Salan and bapen ligands.

complexes containing the methylated bis(aminophenol)-ethylenediamine (bapen) ligands (Figure 2). Bapen ligands are [2,2,2]-type ligands which, upon coordination to a metal center, will form three five-membered chelate rings. This may provide increased stability of the metal complex, compared to one five-membered and two six-membered chelate rings formed with salan-type ligands. Surprisingly, although these bapen compounds have been known for more than 50 years,[34] they have hitherto seen very little application as ligands in metal coordination chemistry and catalysis. A few molybdenum and tungsten dioxo bapen complexes and their oxo transfer ability have been reported,[35,36] and very recently, Okuda and co-workers have reported the application of Group 4 metal complexes containing bapen ligands in olefin polymerization catalysis.[37] Some early and late transition-metal complexes using nonmethylated derivatives have also been reported.[38,39] The structural aspects of these iron(II) salan and bapen complexes in the solid state and in solution have been analyzed by X-ray crystallography and variable-temperature (VT) paramagnetic NMR spectroscopy. The studies have highlighted the importance of careful solution analysis of paramagnetic iron(II) complexes, which can have highly dynamic coordination behavior in solution. Complexes of this type are increasingly investigated as bioinorganic model systems and as nonheme iron-based oxidation catalysts but are often characterized by solid-state methods, such as X-ray diffraction and Mössbauer spectroscopy. As part of our attempts to develop robust homogeneous oxidation catalysts, the reactivity of these complexes toward dioxygen as well as their catalytic potential in oxidation reactions have been investigated.

Experimental Section

All syntheses of complexes were carried out using standard vacuum line, Schlenk, or cannular techniques and stored in a

(19) Hasan, K.; Fowler, C.; Kwong, P.; Crane, A. K.; Collins, J. L.; Kozak, C. M. *Dalton Trans.* **2008**, 2991–2998.
(20) Mialane, P.; Anxolabéhère-Mallart, E.; Blondin, G.; Nivorojkine, A.; Guilhem, J.; Tchertanova, L.; Cesario, M.; Ravi, N.; Bominaar, E. L.; Girerd, J.-J.; Münck, E. *Inorg. Chim. Acta* **1997**, *263*, 367–378.
(21) Strautmann, J. B. H.; DeBeer George, S.; Bothe, E.; Bill, E.; Weyhermüller, T.; Stammler, A.; Bögge, H.; Glaser, T. *Inorg. Chem.* **2008**, *47*, 6804–6824.
(22) Egami, H.; Katsuki, T. *J. Am. Chem. Soc.* **2007**, *129*, 8940–8941.
(23) Glaser, T.; Pawelke, R. H.; Heidemeier, M. *Z. Anorg. Allg. Chem.* **2003**, *629*, 2274–2281.
(24) Pfeiffer, P.; Breith, E.; Lübbe, E.; Tsumaki, T. *Liebigs Ann. Chem.* **1933**, *503*, 84.
(25) Lippard, S. J. *Angew. Chem., Int. Ed. Engl.* **1988**, *27*, 344.
(26) Calvin, M.; Barkelew, C. H. *J. Am. Chem. Soc.* **1946**, *68*, 2267–2273.
(27) Calderazzo, F.; Floriani, C.; Henzi, R.; L'Eplattenier, F. *J. Chem. Soc.* **1969**, *A*, 1378–1386.
(28) Do, L. H.; Lippard, S. J. *Inorg. Chem.* **2009**, *48*, 10708–10719.
(29) Earnshaw, A.; King, E. A.; Larkworthy, L. F. *J. Chem. Soc.* **1968**, *A*, 1048–1052.
(30) Belokon, Y. N.; Fuentes, J.; North, M.; Steed, J. W. *Tetrahedron* **2004**, *60*, 3191–3204.
(31) Hamaker, C. G.; Mirafzal, G. A.; Woo, L. K. *Organometallics* **2001**, *20*, 5171–5176.
(32) Idage, B. B.; Idage, S. B.; Kasegaonkar, A. S.; Jadhav, R. V. *Mater. Sci. Eng., B* **2010**, *168*, 193–198.
(33) Roy, P.; Dhara, K.; Chakraborty, J.; Nethaji, M.; Banerjee, P. *Indian J. Chem.* **2007**, *46A*, 1947–1950.
(34) Freedman, H. H.; Frost, A. E. *J. Org. Chem.* **1958**, *23*, 1292–1298.
(35) Hinshaw, C. J.; Peng, G.; Singh, R.; Spence, J. T.; Enemark, J. H.; Bruck, M.; Kristofzski, J.; Merbs, S. L.; Ortega, R.; Wexler, P. A. *Inorg. Chem.* **1989**, *28*, 4483–4491.
(36) Wong, Y.-L.; Ma, J.-F.; Law, W.-F.; Yan, Y.; Wong, W.-T.; Zhang, Z.-Y.; Mak, T. C. W.; Ng, D. K. P. *Eur. J. Inorg. Chem.* **1999**, 313–321.
(37) Meppelder, G.-J. M.; Fan, H.-T.; Spaniol, T. P.; Okuda, J. *Organometallics* **2009**, *28*, 5159–5165.
(38) Blackmore, K. J.; Lal, N.; Ziller, J. W.; Heyduk, A. F. *J. Am. Chem. Soc.* **2008**, *130*, 2728–2729.
(39) Sik Min, K.; Weyhermüller, T.; Bothe, E.; Wieghardt, K. *Inorg. Chem.* **2004**, *43*, 2922–2931.

nitrogen-filled glovebox. NMR spectra were collected on a Bruker AV-400 or a DRX-400 spectrometer. Chemical shifts for ^{1}H NMR are referenced to the residual protio impurity, and ^{19}F chemical shifts are reported relative to $CFCl_3$. Elemental analysis was performed by the Science Technical Support Unit at London Metropolitan University.

Reagents. The 2-amino-4-fluorophenol was synthesized by nitration of 4-fluorophenol and subsequent reduction of the nitro group.[40] [Fe{N(SiMe$_3$)$_2$}$_2$] was prepared according to a published procedure.[41] The ligands H$_2$salan^{Me}, H$_2$salan^{H}, H$_2$salan^{F}, H$_2$salan^{Cl}, and H$_2$salan^{tBu,tBu} were prepared according to previously reported methods.[42,43] The synthesis for the ligands H$_2$bapen^{H}, H$_2$bapen^{F}, and H$_2$bapen^{Cl} are analogous to the synthesis of the methyl derivative H$_2$bapen^{Me} given below and are provided in the Supporting Information. Similarly, the synthesis for the complexes [Fe(salan^{H})(Py)$_2$], [Fe(salan^{F})(Py)$_2$], [Fe(salan^{Cl})(Py)$_2$], [Fe(bapen^{Me})(Py)$_2$], [Fe(bapen^{H})(Py)$_2$], [Fe(bapen^{F})(Py)$_2$], and [Fe(bapen^{Cl})(Py)$_2$] is analogous to the synthesis of [Fe(salan^{Me})(Py)$_2$] described below and has been included in the Supporting Information. All other reagents are commercially available and were used without further purification.

***N,N′*-Dimethyl-*N,N′*-bis(5-methyl-2-hydroxyphenyl)-1,2-diaminoethane (H$_2$bapen^{Me}).** To a suspension of 2-amino-4-methylphenol (10.0 g, 81.2 mmol) in water (20 mL) was added 1,2-dibromoethane (7.6 g, 40.6 mmol). The mixture was refluxed for 6 h, and the resulting solid was filtered and recrystallized from ethanol to yield H$_4$bapen^{Me} as a brown powder (4.3 g, 39%). ^{1}H NMR (400 MHz, d_6-DMSO, 298 K): δ 8.93 (s, 2H, NH), 6.53 (d, 2H, $^3J_{HH}$ = 7.7, ArH), 6.37 (d, 2H, $^4J_{HH}$ = 1.7, ArH), 6.21 (dd, 2H, $^3J_{HH}$ = 7.7, $^4J_{HH}$ = 1.7, ArH), 4.72 (s, 2H, ArOH), 3.25 (s, 4H, N(CH$_2$CH$_2$)N), 2.12 (s, 2H, ArCH$_3$).

To a solution of H$_4$bapen^{Me} (1.0 g, 3.67 mmol) in tetrahydrofuran (40 mL) at 0 °C was added *n*-butyllithium (2.5 M in hexanes; 8.47 mL, 14.69 mmol). The reaction was stirred for 1 h before being allowed to slowly warm to room temperature. Iodomethane (457 μL, 7.34 mmol) was added slowly, and the solution stirred overnight. The volatiles were removed under reduced pressure, and water (20 mL) was added. The mixture was extracted with dichloromethane (3 × 50 mL), and the extracts were combined and dried over sodium sulfate. The solvent was removed, and the residual solid was washed with methanol to yield a white powder (705 mg, 64%). ^{1}H NMR (400 MHz, d_6-DMSO, 298 K): δ 8.99 (br s, 2H, ArOH), 6.78 (s, 2H, ArH), 6.68−6.57 (m, 4H, ArH), 3.02 (s, 4H, N(CH$_2$CH$_2$)N), 2.66 (s, 6H, NCH$_3$), 2.17 (s, 6H, ArCH$_3$). ^{13}C NMR (400 MHz, d_6-DMSO, 298 K): δ 148.84, 140.01, 127.98, 123.88, 120.96, 115.80 (aromatic C), 54.52 (CH$_2$), 20.94 (CH$_3$). MS (ESI): m/z = 301, [M + H]$^+$. Elemental analysis for C$_{18}$H$_{24}$N$_2$O$_2$ (fw 300.4): C, 71.97; H, 8.05; N, 9.33%. Found C, 72.09; H, 7.94; N, 9.25%.

[Fe(salan^{Me})(Py)$_2$]. To a solution of H$_2$salan^{Me} (400 mg, 1.22 mmol) in toluene (20 mL) was slowly added [Fe{N(SiMe$_3$)$_2$}$_2$] (459 mg, 1.22 mmol) in toluene (10 mL) at −78 °C. With stirring, the solution was allowed to slowly warm to room temperature to yield a faintly colored solution. After stirring at room temperature for 1 h, pentane (40 mL) was added, and the white precipitate was filtered and washed further three times with pentane (3 × 10 mL) to yield a white powder. The solid was then dissolved in toluene (10 mL) and to this solution was added pyridine (5 mL). The solution was stirred for 30 min, and the volatiles were removed. The residual brown solid was washed with pentane (2 × 10 mL) to yield a red powder (481 mg, 73%). ^{1}H NMR (400 MHz, d^8-toluene, 333 K): δ 162.3, 97.4, 87.9, 82.1, 48.4, 28.4, 25.6, 10.4, 9.0, −7.0, −10.2. MS (LSIMS): m/z = 382, [M − 2Py]$^+$. Elemental analysis for C$_{30}$H$_{36}$FeN$_4$O$_2$ (fw 540.5): C, 66.67; H, 6.71; N, 10.37%. Found C, 66.74; H, 6.81; N, 10.48%. μ_{eff} (BM) = 5.17.

[Fe(salan^{tBu,tBu})]. To a solution of H$_2$salan^{tBu,tBu} (613 mg, 1.17 mmol) in toluene (20 mL) was slowly added [Fe{N(SiMe$_3$)$_2$}$_2$] (440 mg, 1.17 mmol) in toluene (10 mL) at −78 °C. With stirring the solution was allowed to slowly warm to room temperature to yield a faintly colored solution. After stirring at room temperature for 1 h, the solvent was removed, and the residue was dried under vacuum overnight to yield a brown powder (641 mg, 95%). ^{1}H NMR (400 MHz, d^6-benzene, 298 K): δ 100.4, 39.3, 37.56, 21.6, 15.8, 5.7, 1.7. MS (LSIMS): m/z = 578, [M]$^+$. Elemental analysis for C$_{34}$H$_{54}$FeN$_2$O$_2$ (fw 578.7): C, 70.57; H, 9.41; N, 4.84%. Found C, 70.48; H, 9.33; N, 4.77%.

[Fe(salan^{tBu,tBu})(THF)$_2$]. The ligand H$_2$salan^{tBu,tBu} (503 mg, 0.96 mmol) and KH (77 mg, 2 equiv) were mixed in degassed THF and left stirring overnight. The mixture was filtered, and the filtrate was added to $FeCl_2$ (121 mg, 1 equiv) in THF. The solution changed color from yellow to eventually brown. After stirring for 1 day, the solution was filtered, and the solvent evaporated under vacuum to leave a brown solid. ^{1}H NMR (400 MHz, CD_3CN, 298 K): 92.7, 75.8, 40.5, 36.29, 35.5, 33.8, 5.98, −3.87. μ_{eff} (BM) = 5.12. Elemental analysis for C$_{42}$H$_{70}$FeN$_2$O$_4$ (fw 722.9): C, 69.79; H, 9.76; N, 3.88%. Found C, 69.89; H, 9.67; N, 3.97%.

[Ru(salan^{tBu,tBu})(CH$_3$CN)$_2$]. To [RuCl$_2$(*p*-cymene)]$_2$ (306 mg, 0.50 mmol) in acetonitrile (10 mL) was added the sodium salt of the ligand, Na$_2$salan^{tBu,tBu}·2THF (713 mg, 1.00 mmol) in acetonitrile (5 mL). The solution was stirred overnight, and the yellow precipitate was collected. Toluene (10 mL) was added to the precipitate, and the mixture was filtered. The filtrate was then treated with pentane until a yellow precipitate formed, which was isolated and precipitated from toluene/pentane twice to yield a yellow powder (273 mg, 39%). ^{1}H NMR (400 MHz, d_8-toluene, 298 K): 7.31 (d, 2H, $^4J_{HH}$ = 2.6, ArH), 6.93 (d, 2H, $^4J_{HH}$ = 2.6, ArH), 3.41 (d, 2H, $^2J_{HH}$ = 11.8, ArCH$_2$N), 3.03 (d, 2H, $^2J_{HH}$ = 11.8, ArCH$_2$N), 2.88 (d, 2H, $^2J_{HH}$ = 8.6, (N(CH$_2$CH$_2$)N)), 2.81 (s, 6H, NCH$_3$), 2.14 (d, 2H, $^2J_{HH}$ = 8.6, (N(CH$_2$CH$_2$)N)), 1.74 (s, 18H, Ar^{t}Bu), 1.47 (s, 18H, Ar^{t}Bu), 1.27 (s, 6H, MeCN). ^{13}C NMR (100 MHz, d_8-toluene, 298 K): 172.42, 138.29, 131.74, 125.74, 122.13, 118.89 (aromatic C), 35.53, 34.10 (quaternary C) 64.46, 60.82 (CH$_2$), 49.56, 32.48, 30.56 (CH$_3$). MS (LSIMS): m/z = 706, [M]$^+$, 663, [M − MeCN]$^+$, 624, [M − 2MeCN]$^+$. Elemental analysis for C$_{38}$H$_{60}$N$_4$O$_2$Ru (fw 706.0): C, 64.65; H, 8.57; N, 7.94%. Found C, 64.49; H, 8.56; N, 7.97%.

X-ray Crystallography. Table 1 provides a summary of the crystallographic data for compounds [Fe(salan^{Cl})(Py)$_2$], [Fe(salan^{H})]$_2$, [{Fe(salan^{Cl})}$_2$(μ-O)], [Fe(bapen^{Cl})(Py)$_2$], [{Fe(salan^{H})(Py)}$_2$(μ-O)] and [{(salan^{Cl})Fe(μ-O,O′-salan^{Cl})Fe}$_2$(μ-O)]. CCDC 789629, 789630, 789631, 789633, 789634 and 789796, respectively.

Results and Discussion

Synthesis of Salan and Bapen Ligands. The synthesis and characterization of the ligands H$_2$salan^{X} used in this study have been reported previously.[42] The bis(aminophenol)ethylenediamine (H$_2$bapen^{X}) ligands were prepared in a two-step procedure, as shown in eq 1. The precursors H$_4$bapen^{X}, prepared from the appropriate

(40) Joshi, A. V.; Baidoosi, M.; Mukhopadhyay, S.; Sasson, Y. *Org. Process Res. Dev.* **2003**, *7*, 95.
(41) Andersen, R. A.; Faegri, K., Jr.; Green, J. C.; Haaland, A.; Lappert, M. F.; Leung, W. P.; Rypdal, K. *Inorg. Chem.* **1988**, *27*, 1782.
(42) Whiteoak, C. J.; Britovsek, G. J. P.; Gibson, V. C.; White, A. J. P. *Dalton Trans.* **2009**, 2337–2344.
(43) Tshuva, E. Y.; Gendeziuk, N.; Kol, M. *Tetrahedron Lett.* **2001**, *42*, 6405–6407.

Table 1. Crystallographic Data for Compounds [Fe(salan^{Cl})(Py)$_2$], [Fe(salan^{H})]$_2$, [{Fe(salan^{Cl})}$_2$(μ -O)], [Fe(bapen^{Cl})(Py)$_2$], [{Fe(salan^{H})(Py)}$_2$(μ -O)], and [{(salan^{Cl})-Fe(μ-O,O′-salan^{Cl})Fe}$_2$(μ-O)]

data	[Fe(salan^{Cl})(Py)$_2$]	[Fe(salan^{H})]$_2$	[{Fe(salan^{Cl})}$_2$(μ -O)]
chemical formula	$C_{28}H_{30}Cl_2FeN_4O_2$	$C_{36}H_{44}Fe_2N_4O_4$	$C_{36}H_{40}Cl_4Fe_2N_4O_5$
solvent	$3C_5H_5N$	CH_3CN	—
fw	818.61	749.51	862.22
T (°C)	−100	−100	−100
space group	*Pccn* (no. 56)	$P2_1/n$ (no. 14)	$P\bar{1}$ (no. 2)
a (Å)	11.7059(2)	11.7368(2)	9.5427(8)
b (Å)	20.5872(4)	17.9168(2)	9.5864(5)
c (Å)	17.0688(3)	18.1254(3)	11.8820(9)
α (deg)	—	—	103.865(6)
β (°)	—	107.1500(17)	93.513(7)
γ (°)	—	—	115.405(7)
V (Å^3)	4113.44(13)	3642.04(10)	936.41(14)
Z	4[a]	4	1[b]
ρ_{calcd} (g cm^{-3})	1.322	1.367	1.529
λ (Å)	0.71073	0.71073	1.54184
μ (mm^{-1})	0.542	0.843	9.230
R_1(obs)[c]	0.0555	0.0343	0.0530
wR_2(all)[d]	0.1826	0.1005	0.1401

data	[Fe(bapen^{Cl})(Py)$_2$]	[{Fe(salan^{H})(Py)}$_2$(μ-O)]	[{(salan^{Cl})Fe(μ-O,O′-salan^{Cl})Fe}$_2$(μ-O)]
chemical formula	$C_{26}H_{26}Cl_2FeN_4O_2$	$C_{46}H_{54}Fe_2N_6O_5$	$C_{72}H_{80}Cl_8Fe_4N_8O_9$
solvent	$2C_5H_5N$	$2C_5H_5N$	$3C_6H_6$
fw	711.46	1040.85	1942.76
T (°C)	−100	−100	−100
space group	$P\bar{1}$ (no. 2)	*Pbcn* (no. 60)	$P2_1/c$ (no.14)
a (Å)	10.8416(2)	18.6514(4)	29.257(4)
b (Å)	12.3542(4)	12.1264(3)	12.9382(9)
c (Å)	14.3132(4)	23.1478(4)	27.262(4)
α (°)	90.566(2)	—	—
β (°)	110.118(2)	—	117.308(17)
γ (°)	107.172(2)	—	—
V (Å^3)	1706.57(9)	5235.44(19)	9170(2)
Z	2	4[a]	4
ρ_{calcd} (g cm^{-3})	1.385	1.321	1.407
λ (Å)	0.71073	1.54184	0.71073
μ (mm^{-1})	0.640	4.888	0.913
R_1[c]	0.0473	0.0324	0.0637
wR_2[d]	0.1554	0.0972	0.1430

[a] The molecule has crystallographic C_2 symmetry. [b] The molecule has crystallographic C_i symmetry. [c] $R_1 = \sigma \||F_o| - |F_c|\|/\sigma |F_o|$. For observed data, $|F_o| > 4\sigma(|F_o|)$. [d] $wR_2 = \{\sigma[w(F_o^2 - F_c^2)^2]/\sigma[w(F_o^2)^2]\}^{1/2}$; $w^{-1} = \sigma^2(F_o^2) + (aP)^2 + bP$.

aminophenol and dibromoethane,[34,44,45] were methylated to give the H$_2$bapen^{X} ligands.[36]

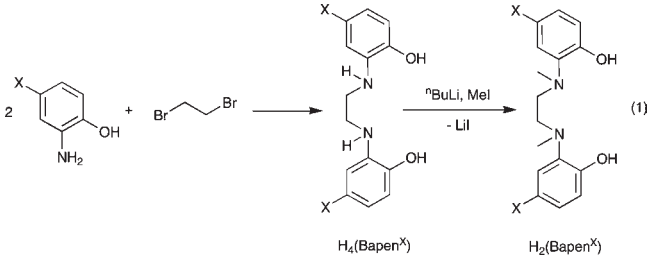

Synthesis of Iron(II) Salan Complexes. Initial attempts to prepare iron(II) complexes of the type [Fe(salan^{X})] were carried out by salt metathesis reactions starting from FeBr$_2$. For example, the reaction of H$_2$salan^{Cl} with two equivalents of KH in THF yields the potassium salt K$_2$salan^{Cl}, which upon reaction with iron(II) bromide in THF yields a brown product. Analysis of this product suggested the formulation of this complex as [Fe(salan^{Cl})(THF)$_2$]. In order to avoid the use of donor solvents, such as THF, an alternative synthesis toward [Fe(salan^{X})] complexes was investigated. Inspired by a recent report on the synthesis of iron(II) phenoxyimine complexes,[46] the iron(II) precursor complex [Fe{N(SiMe$_3$)$_2$}$_2$] was used. The green liquid complex [Fe{N(SiMe$_3$)$_2$}$_2$] was reacted with H$_2$salan^{H} in toluene at room temperature for 1 h, resulting in a color change from green to colorless. The addition of pentane resulted in the precipitation of a white solid, which is poorly soluble in noncoordinating solvents. Addition of an excess of pyridine to a toluene suspension of this white solid resulted in a red-brown solution. The product was precipitated from the toluene/pyridine solution with pentane to yield a brown complex which was characterized as [Fe(salan^{H})(Py)$_2$]. This synthetic methodology, depicted in Scheme 1, enabled the synthesis of a series of iron(II) salan complexes [Fe(salan^{x})(Py)$_2$], where X = H, Me, F, and Cl, which were all fully characterized by elemental analysis, ^{1}H NMR, and MS and, in the case of [Fe(salan^{Cl})-(Py)$_2$], by X-ray crystallography. All complexes are red-brown in color, and magnetic susceptibility measurements (Evans' NMR method) have shown that they are high spin (S = 2) at room temperature. The formation

(44) Vaughan, O. J.; Gibson, J. F. *Polyhedron* **1990**, *9*, 1593–1601.
(45) Ochoa, M. E.; Rojas-Lima, S.; Höpfl, H.; Rodríguez, P.; Castillo, D.; Farfán, N.; Santillan, R. *Tetrahedron* **2001**, *57*, 55–64.
(46) Houghton, J.; Simonovic, S.; Whitwood, A. C.; Douthwaite, R. E.; Carabineiro, S. A.; Yuan, J.-C.; Marques, M. M.; Gomez, P. T. *J. Organomet. Chem.* **2008**, *693*, 717–724.

Scheme 1

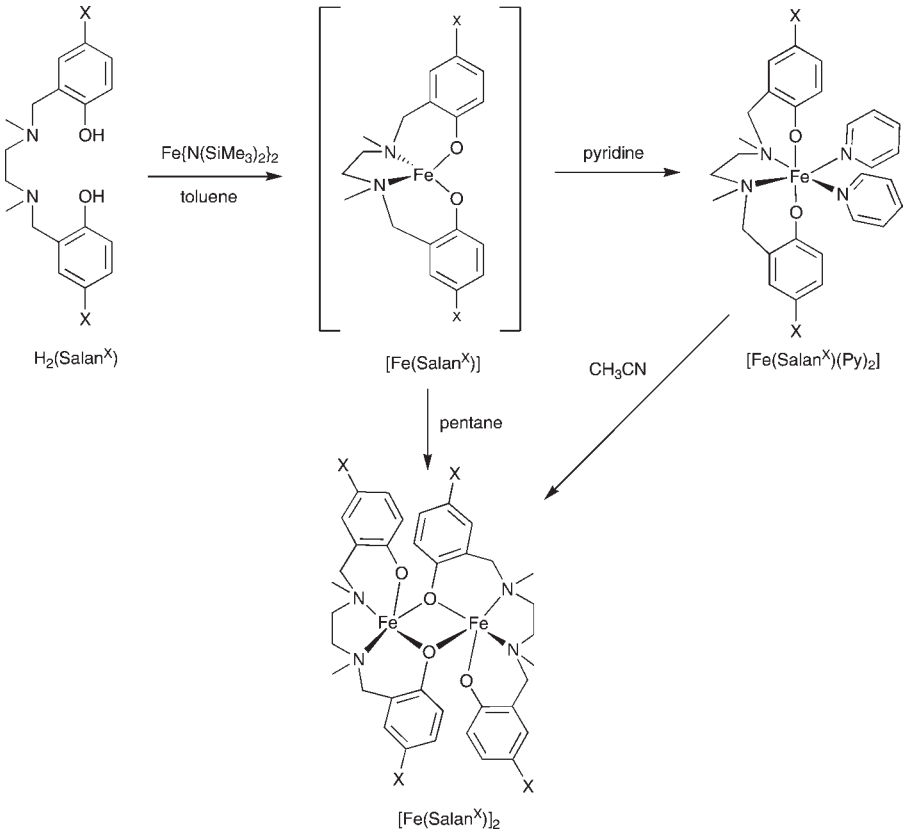

of six-coordinate complexes [Fe(salan^{x})(Py)$_2$] is different compared to iron(II) salen complexes, which form five-coordinate complexes [Fe(salen)(Py)] with only one coordinated pyridine ligand.[27,47,48]

The chloro- and methyl-substituted complexes [Fe(salan^{Cl})(Py)$_2$] and [Fe(salan^{Me})(Py)$_2$] are soluble in acetonitrile. In contrast, the complexes [Fe(salan^{H})(Py)$_2$] and [Fe(salan^{F})(Py)$_2$], when dissolved in acetonitrile at room temperature, form a white precipitate within minutes. This white product can be isolated but is extremely air sensitive and very insoluble; only dissolving in strongly coordinating solvents, such as pyridine. When a solution of complex [Fe(salan^{H})(Py)$_2$] in toluene was layered with acetonitrile, white crystals formed after several days, which were analyzed by X-ray crystallography as a dinuclear phenoxide-bridged complex [Fe(salan^{H})]$_2$ (Scheme 1). It appears that decoordination of the pyridine ligands takes place in acetonitrile, and the formation of a dinuclear phenoxide-bridged complex [Fe(salan^{H})]$_2$ occurs, rather than the formation of a bis(acetonitrile) complex [Fe(salan^{H})(CH$_3$CN)$_2$], analogous to the ruthenium(II) complex [Ru(salan^{tBu,tBu})(CH$_3$CN)$_2$] which we have prepared separately (vide infra).

Dinuclear phenoxide-bridged iron complexes are not uncommon, and several complexes containing salen-type ligands have been reported.[49−51] [Fe(salan^{H})]$_2$ is the first example of a dinuclear phenoxide-bridged iron(II) salan complex. A related complex is a phenoxide-bridged Fe(II) complex featuring two bidentate aminomethylphenolate ligands reported by van Koten and co-workers.[52] Based on the results obtained so far, we postulate that the initial reaction between [Fe{N(SiMe$_3$)$_2$}$_2$] and H$_2$salan^{X} in toluene results in the formation of a tetrahedral complex of the type [Fe(salan^{X})] or possibly an octahedral complex containing weakly coordinating NH(SiMe$_3$)$_2$ ligands, [Fe(salan^{X}){NH(SiMe$_3$)$_2$}$_2$], which are soluble in toluene. Addition of pentane results in the precipitation of the white dinuclear phenoxide-bridged complexes [Fe(salan^{X})]$_2$. These white complexes are identical to the white complexes that precipitate from a solution of [Fe(salan^{X})(Py)$_2$] in toluene upon the addition of acetonitrile (Scheme 1).

In order to prepare mononuclear iron(II) salan complexes [Fe(salan)], the sterically encumbered *ortho*- and *para*-*tert*-butyl substituted salan ligand H$_2$salan^{tBu,tBu} was employed (Scheme 2). This ligand was first used by Kol and co-workers for Group 4 metal complexes.[43] The additional steric bulk in the ortho positions prevents the formation of phenoxide-bridged dinuclear complexes. The reaction of H$_2$salan^{tBu,tBu} with [Fe{N(SiMe$_3$)$_2$}$_2$] in toluene resulted in a brown complex, which according to mass spectrometry and CHN analysis corresponds to [Fe(salan^{tBu,tBu})]. Unlike the dinuclear white complexes [Fe(salan^{X})]$_2$, this complex is highly soluble, even in nonpolar solvents, such as pentane. The structure of this iron(II)

(47) Niswander, R. H.; Martell, A. E. *Inorg. Chem.* **1978**, *17*, 2341–2344.
(48) Wiznycia, A. V.; Desper, J.; Levy, C. J. *Inorg. Chem.* **2006**, *45*, 10034–10036.
(49) Scheringer, C.; Hinkler, K.; von Stackelberg, M. *Z. Anorg. Allg. Chem.* **1960**, *306*, 35–38.
(50) Gerloch, M.; Mabbs, F. E. *J. Chem. Soc.* **1967**, *A*, 1900–1908.
(51) Smith, A. L.; Day, C. S.; Que, L., Jr.; Zhou, Y.; Bierbach, U. *Inorg. Chim. Acta* **2007**, *360*, 2824–2828.
(52) Brandts, J. A. M.; Janssen, M. D.; Hogerheide, M. P.; Boersma, J.; Spek, A. L.; van Koten, G. *Inorg. Chim. Acta* **1999**, *291*, 326–332.

Scheme 2

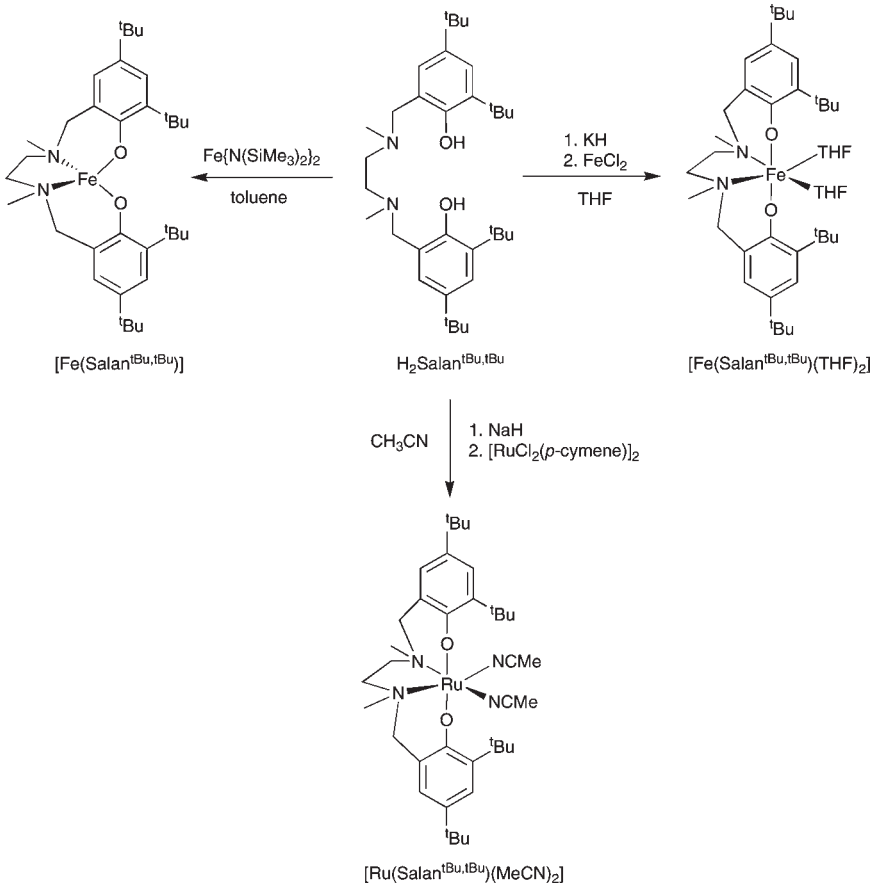

complex is presumed to be tetrahedral, similar to the tetrahedral iron(II) complexes with bidentate salicylaldimine ligands[46,53] and the analogous tetrahedral zinc(II) complex [Zn(salan^{tBu,tBu})], which was recently reported.[54] The reaction of H$_2$salan^{tBu,tBu} with two equivalents of KH results in the dipotassium salt K$_2$salan^{tBu,tBu}, which can subsequently be reacted with FeCl$_2$ in THF to give the complex [Fe(salan^{tBu,tBu})(THF)$_2$] (Scheme 2).

Extensions to Fe(III) and Ru(II) have also been investigated. The reaction of K$_2$salan^{tBu,tBu} with FeCl$_3$ in THF results in the formation of the dark-purple complex [Fe(salan^{tBu,tBu})Cl] (see Supporting Information, Figure S9), which was also reported by Kozak and co-workers.[19] The synthesis of a ruthenium(II) salan complex was carried out by reacting Na$_2$salan^{tBu,tBu} with [RuCl$_2$(*p*-cymene)]$_2$ in acetonitrile. This resulted in the isolation of the first ruthenium(II) salan complex [Ru(salan^{tBu,tBu})(MeCN)$_2$], which is a diamagnetic yellow solid and was characterized by NMR, MS, and CHN analysis (Scheme 2).

Synthesis of Iron bapen Complexes. Iron(II) complexes containing the tetradentate dianionic bapen^X ligands can be prepared in a similar fashion as the salan^X complexes. The combination of [Fe{N(SiMe$_3$)$_2$}$_2$] and H$_2$bapen^X in toluene, followed by the addition of pentane, results in a white precipitate. This intermediate is presumed to be either a monomeric four-coordinate complex [Fe(bapen^X)] or a phenoxide-bridged dinuclear complex [Fe(bapen^X)]$_2$, in analogy to the [Fe(salan^X)]$_2$ complexes. Subsequent addition of pyridine results in the formation of a series of iron(II) complexes [Fe(bapen^X)(Py)$_2$], where X = H, Me, F, and Cl (eq 2). These complexes have been fully characterized by ^{1}H NMR, MS, elemental analysis, and magnetic susceptibility measurements and, in the case of [Fe(bapen^{Cl})(Py)$_2$], by X-ray crystallography. All complexes have magnetic moments at room temperature typical for high-spin iron(II) complexes.

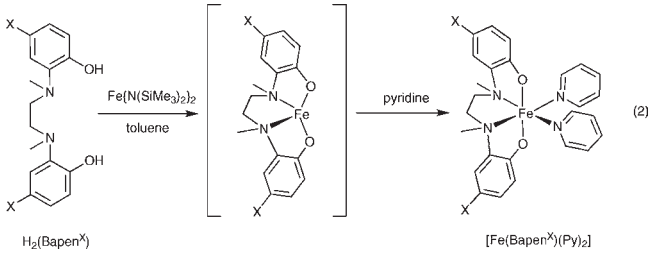

(2)

Oxidation Reactions and Reactivity Toward Dioxygen. The iron(II) salan^X and bapen^X complexes prepared in this study were applied as catalysts for the oxidation of cyclohexane with H$_2$O$_2$ under our standard conditions (see Supporting Information). No oxidation products (cyclohexanol or cyclohexanone) were obtained under these conditions. During the course of these studies, it was noticed that the iron(II) salan and bapen complexes are very reactive toward dioxygen. Initially, it was suspected that the salan ligands could be susceptible to

(53) Torzilli, M. A.; Colquhoun, S.; Kim, J.; Beer, R. H. *Polyhedron* **2002**, *21*, 705–713.
(54) Dong, Q.; Ma, X.; Guo, J.; Wei, X.; Zhou, M.; Liu, D. *Inorg. Chem. Commun.* **2008**, *11*, 608–611.

oxidative degradation upon exposure of the complexes to an oxidant, whereby the C−N bonds are oxidized (dehydrogenated) to C=N bonds, essentially converting the salan ligand into a salen ligand as has been seen previously.[17,55] However, when a solution of the complex [Fe(salan^{Cl})(THF)$_2$] is exposed to air, an oxidation reaction takes place to give the oxo-bridged dinuclear Fe(III) complex [{Fe(salan^{Cl})}$_2$(μ-O)], which was characterized by X-ray crystallography (eq 3). Oxo-bridged dinuclear iron(III) complexes of the type [LFe−O−FeL] are very common, but this is only the second example featuring salan ligands.[23] Interestingly, on one occasion during the preparation of [{Fe(salan^{Cl})}$_2$(μ-O)], crystals were obtained from a benzene solution after exposure to air, which were shown by X-ray analysis to be a tetranuclear mixed iron(II)/iron(III) complex [{(salan^{Cl})Fe(μ-O,O′-salan^{Cl})-Fe}$_2$(μ-O)] (see eq 3). This tetranuclear structure, although of insufficient quality to be analyzed and reported in detail (see Supporting Information), clearly shows a central core of the oxo-bridged dinuclear complex [{Fe^{III}(salan^{Cl})}$_2$-(μ-O)] with two [Fe^{II}(salan^{Cl})] units attached by two bridging phenolate moieties. This tetranuclear complex can be viewed as a halfway intermediate in the oxidation pathway starting from the dinuclear iron(II) salan complex toward the oxidized dinuclear iron(III) product [{Fe(III)(salan^{Cl})}$_2$O] (eq 3).

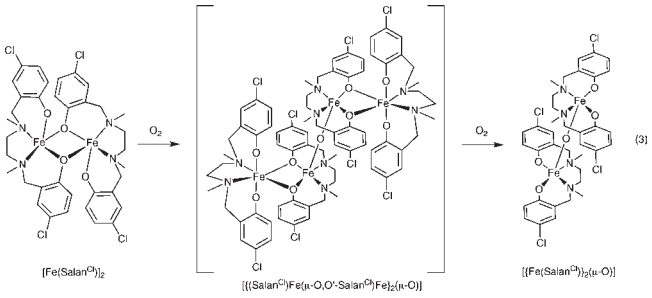

Exposure of the complexes [Fe(salan^{tBu,tBu})(THF)$_2$] and [Fe(salan^{tBu,tBu})] to air resulted in both cases in the formation of the known oxo-bridged dinuclear Fe(III) complex [{Fe(salan^{tBu,tBu})}$_2$(μ-O)], which was characterized by X-ray crystallography (see eq 4 and Supporting Information, Figure S5). This oxo-bridged complex was previously reported by Glaser and co-workers, prepared via a different route from the Fe(III) precursor Fe(NO$_3$)$_3$, H$_2$salan^{tBu,tBu} and NEt$_3$.[23]

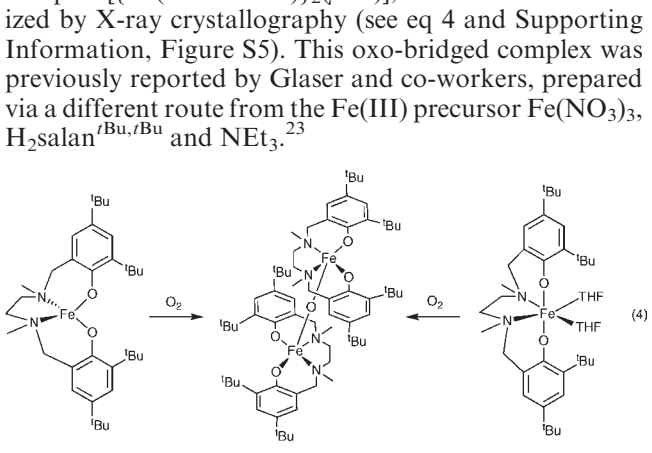

The complex [Fe(salan^{H})(Py)$_2$], containing the stronger coordinating pyridine ligands, also oxidizes upon exposure to air to give the oxo-bridged iron(III) complex [{Fe-(salan^{H})(Py)}$_2$(μ-O)] (see eq 5).

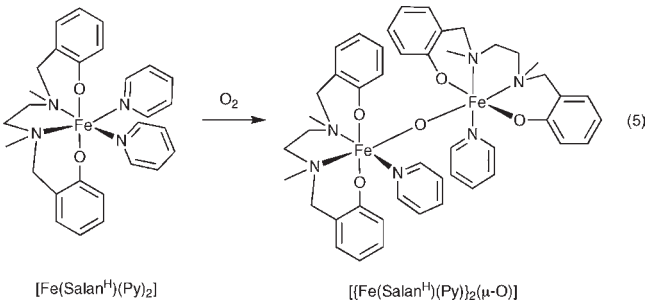

In our previous studies on iron(II) complexes with neutral tetradentate ligands,[56] we have shown that the coordination geometry in solution of these complexes can be highly dynamic, resulting in temperature-dependent equilibria between species with different coordination geometries. Crystallization of the complexes and the determination of the structure in the solid state provides important information for their characterization but gives no information about their behavior in solution. Additional solution studies by variable temperature NMR are essential to fully understand the dynamic behavior of these complexes. In the next sections, we will first discuss the solid-state structures before discussing their solution behavior.

Solid-State Structures

The solid-state structure of [Fe(salan^{H})]$_2$ shows the dinuclear complex with the two [Fe(salen^{H})] units bridged by one phenoxide donor atom from each ligand (see Figure 3 and Table 2). The geometry at each iron center is slightly distorted square-based pyramidal [τ = 0.10 at Fe(1) and 0.13 at Fe(2)] with O(18) and O(38) occupying the apical sites at Fe(1) and Fe(2), respectively. The central Fe$_2$O$_2$ ring adopts a rhomboid geometry; the ring is flat (the four atoms are coplanar to better than 0.01 Å), the Fe−O bonds are essentially the same (lying in the narrow range 2.0662(10) to 2.0726(10) Å), and the opposite angles are likewise the same (those at Fe(1) and Fe(2) are 73.58(4) and 73.60(4)° respectively, while those at O(1) and O(21) are 106.30(4) and 106.51(4)° respectively).

Linear tetradentate ligands can adopt three coordination topologies in octahedral metal complexes: cis-α, cis-β, and trans.[57] The two internal amine donors become chiral upon coordination to the metal center and can therefore have either the same or opposite configuration. Assuming that the configuration of these two donors remains unchanged, the number of possible topological isomers increases to five pairs of enantiomers: cis-α (*R**,*R**), cis-β (*R**,*R**) or cis-β (*R**,*S**), and trans (*R**,*R**) or trans (*R**,*S**), whereby *R** and *S** denote the relative configuration at the internal donor atoms.[56] From molecular models it is immediately evident that the cis-α (*R**,*S**) topology is not possible due to severe bite-angle strain within the complex. Whichever topology a linear tetradentate ligand will adopt preferentially in a metal complex is not easily predicted and depends on a number of

(55) Böttcher, A.; Elias, H.; Jäger, E.-G.; Langfelderova, H.; Mazur, M.; Müller, L.; Paulus, H.; Pelikan, P.; Rudolph, M.; Valko, M. *Inorg. Chem.* **1993**, *32*, 4131–4138.

(56) England, J.; Davis, C. R.; Banaru, M.; White, A. J. P.; Britovsek, G. J. P. *Adv. Synth. Catal.* **2008**, *350*, 883–897.

(57) Gavrilova, A. L.; Bosnich, B. *Chem. Rev.* **2004**, *104*, 349–383.

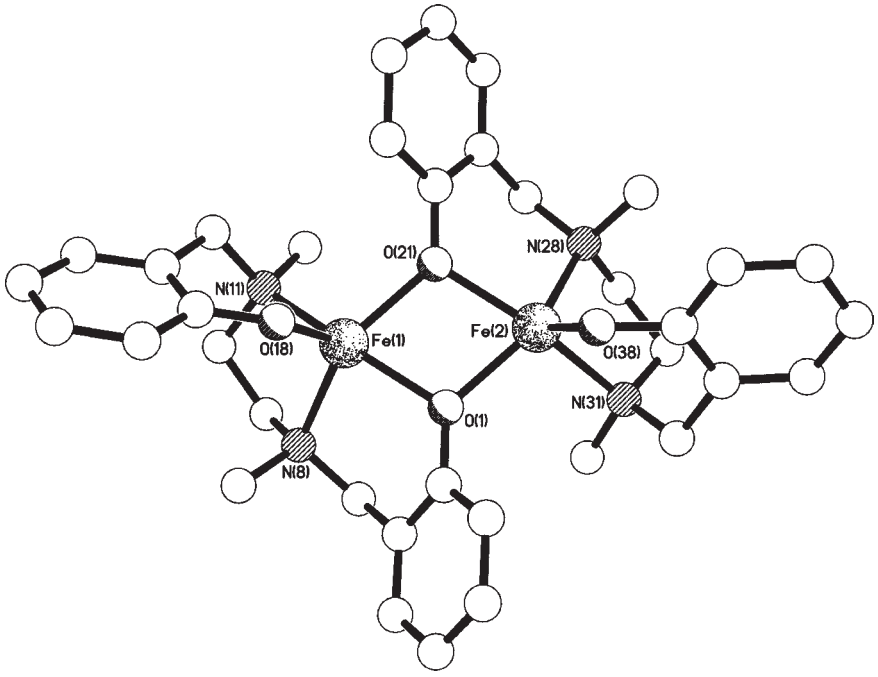

Figure 3. The molecular structure of complex $[Fe(salan^{H})]_2$.

Table 2. Selected Bond Lengths (Å) and Angles (°) for $[Fe(salan^{H})]_2$

Fe(1)−O(1)	2.0693(10)	Fe(1)−N(8)	2.2369(12)
Fe(1)−N(11)	2.2172(12)	Fe(1)−O(18)	1.9153(11)
Fe(1)−O(21)	2.0702(10)	Fe(2)−O(1)	2.0726(10)
Fe(2)−O(21)	2.0662(10)	Fe(2)−N(28)	2.2264(12)
Fe(2)−N(31)	2.2343(13)	Fe(2)−O(38)	1.9257(11)
O(1)−Fe(1)−N(8)	86.31(4)	O(1)−Fe(1)−N(11)	148.76(5)
O(1)−Fe(1)−O(18)	118.52(5)	O(1)−Fe(1)−O(21)	73.58(4)
N(8)−Fe(1)−N(11)	80.17(4)	N(8)−Fe(1)−O(18)	108.66(5)
N(8)−Fe(1)−O(21)	142.53(4)	N(11)−Fe(1)−O(18)	92.55(5)
N(11)−Fe(1)−O(21)	100.86(4)	O(18)−Fe(1)−O(21)	108.70(5)
O(1)−Fe(2)−O(21)	73.60(4)	O(1)−Fe(2)−N(28)	141.80(4)
O(1)−Fe(2)−N(31)	100.72(4)	O(1)−Fe(2)−O(38)	107.21(5)
O(21)−Fe(2)−N(28)	86.59(4)	O(21)−Fe(2)−N(31)	149.64(4)
O(21)−Fe(2)−O(38)	117.50(4)	N(28)−Fe(2)−N(31)	80.12(4)
N(28)−Fe(2)−O(38)	110.90(5)	N(31)−Fe(2)−O(38)	92.78(4)
Fe(1)−O(1)−Fe(2)	106.30(4)	Fe(1)−O(21)−Fe(2)	106.51(4)

factors, including the number of atoms between the donors, the solvent, and the temperature. In addition, if complexes are labile, equilibria can exist between different topological isomers in solution, which will be concentration and temperature dependent. The topology of the isomer observed by X-ray crystallography in the solid state is only partly representative of what is present in solution. This was previously shown to be the case for other high-spin iron(II) complexes containing tetradentate bis(pyridylmethyl)diamine and bis(quinolyl)-diamine ligands.[56,58,59]

The order of stability for tetradentate [3,2,3]-type ligands, such as the salan ligands used here (the numbers refer to the number of bridging atoms between the donor atoms), is generally as follows: trans (*R**,*R**) > cis-β (*R**,*R**) > cis-β (*R**,*S**) > trans (*R**,*S**) ≫ cis-α (*R**,*R**).[57] The trans (*R**,*R**) topology is observed in several five- and six-coordinate Fe(III) complexes containing salan ligands.[60,61] Therefore, in the case of the octahedral $[Fe(salan^{X})(Py)_2]$ complexes, the trans (*R**, *R**) topology was expected. Surprisingly, in the solid-state structure of $[Fe(salan^{Cl})(Py)_2]$, the tetradentate ligand adopts the cis-α (*R**,*R**) coordination mode, with the two pyridine ligands being coordinated cis to each other (Figure 4 and Table 3). As will be seen in the next section, this is not the only topology observed in solution at room temperature, but it appears to be the one that crystallizes preferentially.

The order of stability for tetradentate [2,2,2]-type ligands such as the bapen ligands used here, is as follows: cis-α (*R**,*R**) > cis-β (*R**,*R**) > cis-β (*R**,*S**) > trans (*R**,*R**) ≫ trans (*R**,*S**).[57] The cis-α (*R**,*R**) topology is indeed the only coordination mode observed for bapen ligands so far.[35−37] In the case of complex $[Fe(bapen^{Cl})(Py)_2]$, the molecular structure in the solid state shows the expected cis-α (*R**,*R**) topology (Figure 5 and Table 4). However, as will be seen in the next section, the cis-α (*R**,*R**) topology is not the only one present in solution, especially at elevated temperatures.

The molecular structure of the iron(III) oxo-bridged complex $[\{Fe(salan^{Cl})\}_2(\mu\text{-O})]$ is shown in Figure 6. The structure of $[\{Fe(salan^{Cl})\}_2(\mu\text{-O})]$ was found to be severely disordered with two orientations being identified for every atom except for the iron and the bridging oxygen atoms (see Figure S4, Supporting Information). The disorder is likely to be due to the presence of a mixture of the trans (*R**,*S**) and the trans (*R**,*R**) topologies. Such mixtures of isomers in the solid state were also seen in the structure of $[Fe(salan^{Me,tBu})Cl]$.[20] As a consequence of the disorder, little can be said about this structure of $[\{Fe(salan^{Cl})\}_2(\mu\text{-O})]$, other than that the complex is the oxo-bridged dinuclear complex shown in Figure 6, with a trans-coordination mode for the $salan^{Cl}$ ligands, and that the coordination geometry at the iron center is distorted square-based pyramidal (τ = 0.29), with the bridging oxygen in the apical position and the two $salen^{Cl}$ ligands in an anti

(58) Mas-Ballesté, R.; Costas, M.; van den Berg, T.; Que, L., Jr. *Chem.—Eur. J.* **2006**, *12*, 7489–7500.
(59) England, J.; Britovsek, G. J. P.; Rabadia, N.; White, A. J. P. *Inorg. Chem.* **2007**, *46*, 3752–3767.
(60) Lanznaster, M.; Neves, A.; Bortoluzzi, A. J.; Assumpcao, A. M. C.; Vencato, I.; Machado, S. P.; Drechsel, S. M. *Inorg. Chem.* **2006**, *45*, 1005–1011.
(61) Setyawati, I. A.; Rettig, S. J.; Orvig, C. *Can. J. Chem.* **1999**, *77*, 2033–2038.

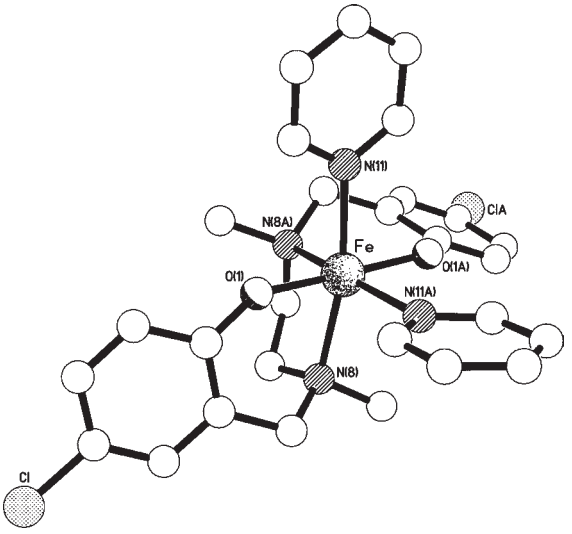

Figure 4. The molecular structure of the C_2-symmetric complex [Fe(salan^{Cl})(Py)$_2$].

Table 3. Selected Bond Lengths (Å) and Angles (°) for [Fe(salan^{Cl})(Py)$_2$]

Fe−O(1)	2.0027(16)	Fe−N(8)	2.2859(18)
Fe−N(11)	2.2460(18)		
O(1)−Fe−N(8)	85.24(6)	O(1)−Fe−N(11)	85.73(7)
O(1)−Fe−O(1A)	175.46(9)	O(1)−Fe−N(8A)	98.30(7)
O(1)−Fe−N(11A)	91.05(7)	N(8)−Fe−N(11)	168.98(7)
N(8)−Fe−N(8A)	78.46(9)	N(8)−Fe−N(11A)	96.62(7)
N(11)−Fe−N(11A)	89.86(10)		

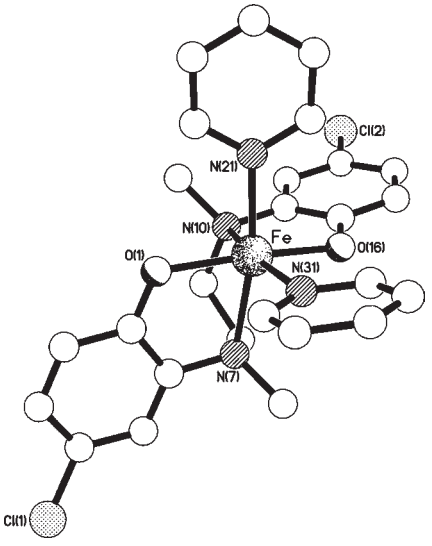

Figure 5. The molecular structure of complex [Fe(bapen^{Cl})(Py)$_2$].

conformation with respect to each other. The Fe−O distance is 1.7793(8) Å, and the Fe−O−FeA angle is 180°.

The single crystal X-ray diffraction data for [{(salan^{Cl})-Fe(μ-O,O′-salan^{Cl})Fe}$_2$(μ-O)] are of insufficient quality to justify a detailed analysis of the structure (see Supporting Information). However, the structural motif as shown in Figure 7 is believed to be correct and has been included in this report because it provides an interesting insight into the stepwise nature of the oxidation of dinuclear iron(II) complexes to oxo-bridged dinuclear iron(III) complexes.

X-ray analysis of crystals of the product [{Fe(salan^{H})-(Py)}$_2$(μ-O)], obtained from the reaction between [Fe-

Table 4. Selected Bond Lengths (Å) and Angles (°) for [Fe(bapen^{Cl})(Py)$_2$]

Fe−O(1)	2.0189(12)	Fe−N(7)	2.2798(14)
Fe−N(10)	2.3183(14)	Fe−O(16)	2.0147(11)
Fe−N(21)	2.1874(14)	Fe−N(31)	2.2086(15)
O(1)−Fe−N(7)	79.30(5)	O(1)−Fe−N(10)	93.69(5)
O(1)−Fe−O(16)	170.24(5)	O(1)−Fe−N(21)	92.40(5)
O(1)−Fe−N(31)	97.75(5)	N(7)−Fe−N(10)	80.04(5)
N(7)−Fe−O(16)	93.12(5)	N(7)−Fe−N(21)	170.43(5)
N(7)−Fe−N(31)	97.65(5)	N(10)−Fe−O(16)	78.83(5)
N(10)−Fe−N(21)	95.90(5)	N(10)−Fe−N(31)	167.72(5)
O(16)−Fe−N(21)	94.59(5)	O(16)−Fe−N(31)	89.30(5)
N(21)−Fe−N(31)	88.11(5)		

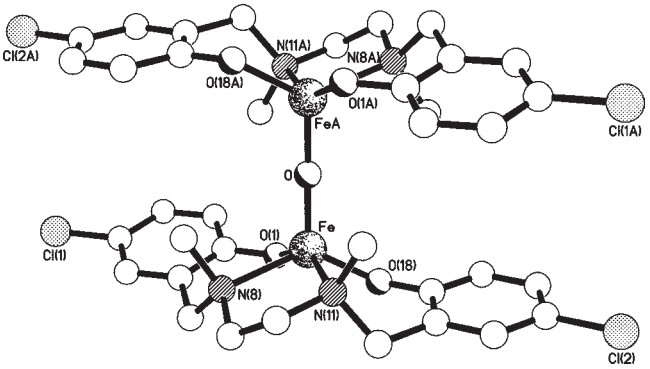

Figure 6. The molecular structure of the C_i-symmetric complex [{Fe(salan^{Cl})}$_2$(μ-O)].

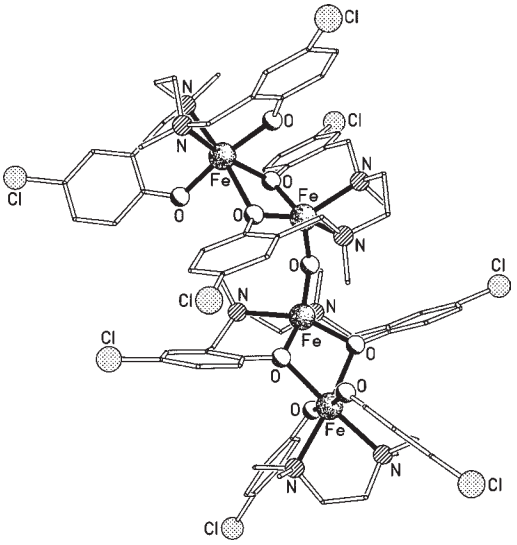

Figure 7. The molecular structure of complex [{(salan^{Cl})Fe(μ-O,O′-salan^{Cl})Fe}$_2$(μ-O)].

(salan^{H})(Py)$_2$] and dioxygen, revealed the formation of a C_2-symmetric oxo-bridged dinuclear complex (Figure 8 and Table 5). The C_2 axis passes through the bridging oxygen atom and bisects the Fe−O−FeA angle. The geometry at the iron center is distorted octahedral with cis angles in the range 77.49(6)−99.66(6)° and with the salen^{H} ligand coordinated in a cis-α (*R**,*R**) fashion. The angle at the bridging oxygen atom is 175.68(12)°.

NMR Spectroscopy

All iron(II) complexes reported here containing salan and bapen ligands are high-spin complexes at room temperature, giving rise to paramagnetic NMR spectra. The combination of the weak-field amine and phenoxide donors and the

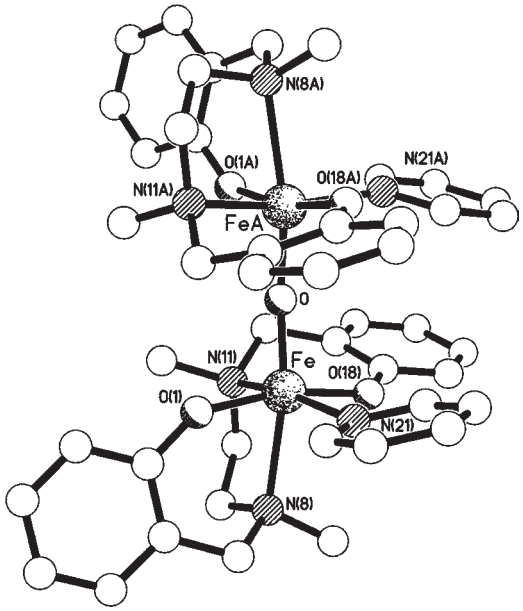

Figure 8. The molecular structure of the C_2-symmetric complex [{Fe(salan^{H})(Py)}$_2$(μ-O)].

Table 5. Selected Bond Lengths (Å) and Angles (°) for [{Fe(salan^{H})(Py)}$_2$(μ-O)]

Fe−O	1.7840(3)	Fe−O(1)	1.9560(13)
Fe−N(8)	2.3981(16)	Fe−N(11)	2.2259(15)
Fe−O(18)	1.9643(13)	Fe−N(21)	2.2255(16)
O−Fe−O(1)	92.89(6)	O−Fe−N(8)	169.77(7)
O−Fe−N(11)	95.04(6)	O−Fe−O(18)	99.66(6)
O−Fe−N(21)	94.94(6)	O(1)−Fe−N(8)	81.00(5)
O(1)−Fe−N(11)	95.26(6)	O(1)−Fe−O(18)	167.32(6)
O(1)−Fe−N(21)	91.15(6)	N(8)−Fe−N(11)	77.49(6)
N(8)−Fe−O(18)	86.84(6)	N(8)−Fe−N(21)	93.37(6)
N(11)−Fe−O(18)	85.54(6)	N(11)−Fe−N(21)	167.84(6)
O(18)−Fe−N(21)	85.95(6)	Fe−O−FeA	175.68(12)

two stronger field pyridine ligands does not provide a strong enough ligand field to generate low-spin complexes or spin-crossover behavior. In this study, VT ^{1}H and ^{19}F NMR spectroscopy has been used to investigate the geometries of the iron(II) salan and bapen complexes in solution.

Fe(II) Complexes Containing Salan Ligands. The VT ^{19}F NMR spectra for complex [Fe(salan^{F})(Py)$_2$], recorded in d^8-toluene, show a major signal at 273 K at −64 ppm and a minor signal at −50 ppm ((Figure 9). The major signal shifts to a lower field at lower temperatures due to Curie behavior. This signal is tentatively assigned to the isomer with the C_2-symmetric trans (*R**,*R**) topology, where the pyridine ligands are in trans position to each other. Although the solid-state structure of the analogous chloro-substituted complex [Fe(salan^{Cl})(Py)$_2$] showed the cis-α (*R**,*R**) topology, this assignment is preferred for several reasons. For [3,2,3]-type tetradentate ligands, the most stable coordination mode is generally the trans (*R**,*R**) topology,[57] and this is also the topology observed in the solid-state structure of a related Fe(III) salan complex.[61] Furthermore, in the case of the less-constrained complex reported by van Koten and co-workers with two bidentate aminomethylphenoxide ligands, the pyridine ligands are trans to each other.[52] The minor peak observed at −50 ppm, which turns into two signals at lower temperatures, can be assigned to the unsymmetrical cis-β (*R**,*R**) isomer. The cis-β (*R**,*R**) coordination mode has been seen

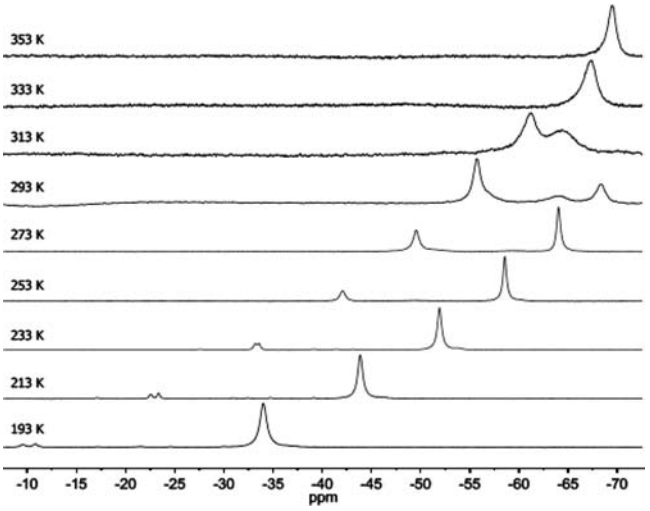

Figure 9. VT ^{19}F NMR spectra of complex [Fe(salan^{F})(Py)$_2$] in d^8-toluene.

previously in several octahedral iron(III) salan complexes, where the formation of the trans (*R**,*R**) topology is not possible either through the formation of dinuclear complexes of the type [LFe(III)-(μ-OR)$_2$-LFe(III)][14,16−18] or by using an additional bidentate ligand.[20] At 293 K, a third species is observed at −63 ppm, which is assigned as the cis-α (*R**,*R**) isomer. Heating the toluene solution to 353 K results in a single broad peak, which most likely represents an average of the three geometries, due to a rapid interconversion between the three topologies, as illustrated in Scheme 3. Alternatively, the formation of a stable five-coordinate complex [Fe(salan^{F})(Py)] at higher temperatures cannot be excluded at this stage, although the chemical shift for this complex would be expected to be different.

The mechanism for the interconversion between the different isomers is believed to involve the dissociation of one of the pyridine ligands. This possible dissociation of a pyridine ligand was investigated by measuring the VT ^{19}F NMR spectra of complex [Fe(salan^{F})(Py)$_2$] in d^5-pyridine over the temperature range from 243 to 343 K. Only one single peak is observed which shifts from −57 ppm at 243 K to −79 ppm at 343 K due to Curie behavior (see Supporting Information, Figure S12). These chemical shift values are essentially the same as those for the major species observed in d^8-toluene (see Figure 9), and the complex present in d^5-pyridine is therefore most likely the isomer with the C_2-symmetric trans (*R**,*R**) topology. The presence of a large excess of pyridine suppresses the formation of other isomers, which strongly suggests that the interconversion between the different isomers observed in toluene involves the dissociation of at least one of the pyridine ligands.

Assuming that the solution behavior for [Fe(salan^{F})-(Py)$_2$] is representative for the other complexes of the type [Fe(salan^{X})(Py)$_2$], these complexes will all exist as mixtures of the three isomers trans (*R**,*R**), cis-β (*R**,*R**), and cis-α (*R**,*R**) in solution. In the case of complex [Fe(salan^{Cl})(Py)$_2$], the cis-α (*R**,*R**) isomer crystallized preferentially to the other isomers under the conditions used, and this was the structure determined in the solid state (Figure 4). It is interesting to note that neither the trans (*R**,*S**) nor the cis-β (*R**,*S**) topology appears to be

Scheme 3

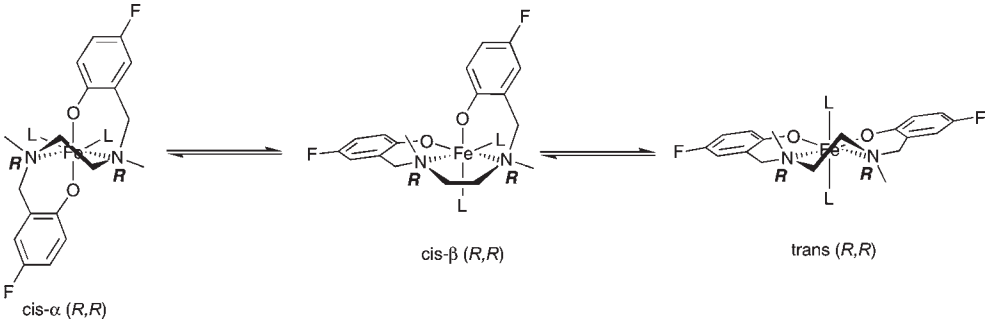

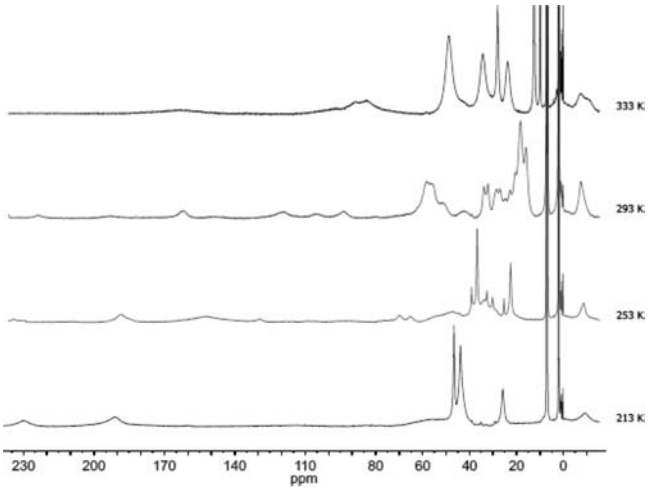

Figure 10. VT ^{1}H NMR spectra of complex [Fe(salen^{F})(Py)$_2$] in d^8-toluene.

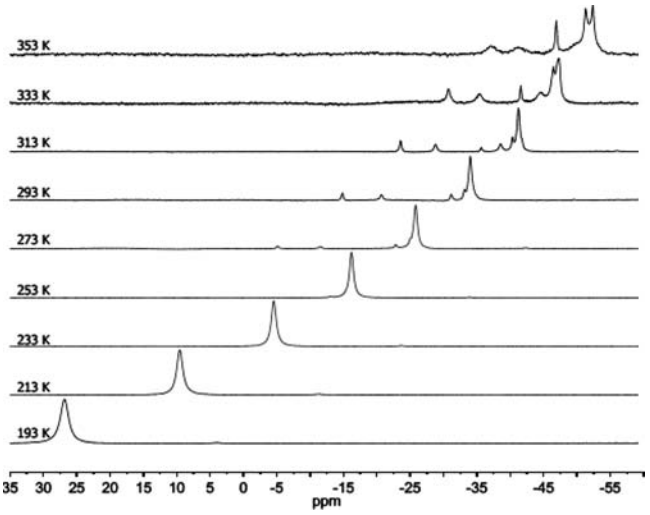

Figure 11. VT ^{19}F NMR spectra of complex [Fe(bapen^{F})(Py)$_2$] in d^8-toluene.

present. Interconversion between (*R**,*R**) and (*R**,*S**) isomers would require an inversion of the configuration at the amine donors, which does not appear to occur for these salan complexes.

The ^{1}H NMR spectrum of [Fe(salan^{F})(Py)$_2$] in d^8-toluene at room temperature is complicated due to existence of several isomers (see Figure 10). However, at 213 K, the spectrum becomes remarkably simple, showing ca. eight signals, as expected for the C_2-symmetric trans (*R**,*R**) isomer. Also at higher temperature (333 K), the spectrum appears to simplify due to a fast interconversion between the three different isomers.

Fe(II) Complexes Containing Bapen Ligands. In the VT ^{19}F NMR spectra of complex [Fe(bapen^{F})(Py)$_2$] in d^8-toluene, only one signal is observed below 273 K, which is tentatively assigned to the cis-α (*R**,*R**) geometry (see Figure 11). This is the geometry seen in the solid-state structure of the analogous chloro-substituted complex [Fe(bapen^{Cl})(Py)$_2$] (see Figure 5), and it is generally the most stable geometry for [2,2,2]-type ligands, where the order of stability is: cis-α (*R**,*R**) > cis-*β* (*R**,*R**) > cis-*β* (*R**,*S**) > trans (*R**,*R**) ≫ trans (*R**,*S**).[57] Above 273 K, other isomers appear, initially the two unsymmetrical cis-*β* (*R**,*R**) and cis-*β* (*R**,*S**) isomers (giving rise to two signals each) and further increase of the temperature reveals another isomer (at ca. −36 ppm at 313 K), most likely the C_2-symmetric trans (*R**,*R**) isomer. The C_s-symmetric trans (*R**,*S**) topology is not observed, as this is the least stable topology for [2,2,2]-type ligands. All possible topologies and their interconversions are illustrated in Scheme 4.

The VT ^{19}F NMR spectra of complex [Fe(bapen^{F})(Py)$_2$] have also been measured in d^5-pyridine over the temperature range from 243 to 343 K. A single peak is observed which shifts from −10 ppm at 243 K to −47 ppm at 343 K due to Curie behavior (see Supporting Information, Figure S13). These chemical shift values are essentially the same as those for the major species observed in d^8-toluene (see Figure 11). The only complex observed in d^5-pyridine is therefore the isomer with cis-α (*R**,*R**) topology. The presence of a large excess of pyridine prevents the formation of other isomers, and we conclude that for both the iron(II) salan and bapen complexes, the interconversion between different isomers in toluene occurs via a dissociative mechanism involving the dissociation of one of the pyridine ligands. The presence of both (*R**,*R**) and (*R**,*S**) isomers in the case of this bapen complex suggests that an inversion of configuration at the nitrogen donor centers can occur. It is possible that the weaker basicity of anilines versus amines renders inversion of configuration more facile for the aniline nitrogen donors in the bapen ligands compared to the amine nitrogen donors in the salan ligands.

VT-^{1}H NMR spectra in d^8-toluene below 273 K show approximately eight signals, which indicates the presence of a single isomer, most likely with cis-α (*R**,*R**) topology (Figure 12). Some of the signals are rather broad, and full

Scheme 4

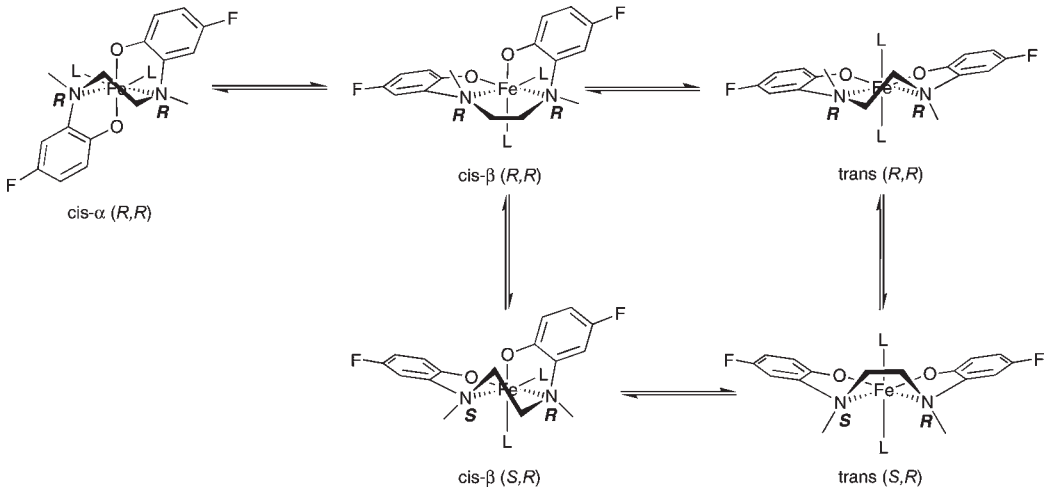

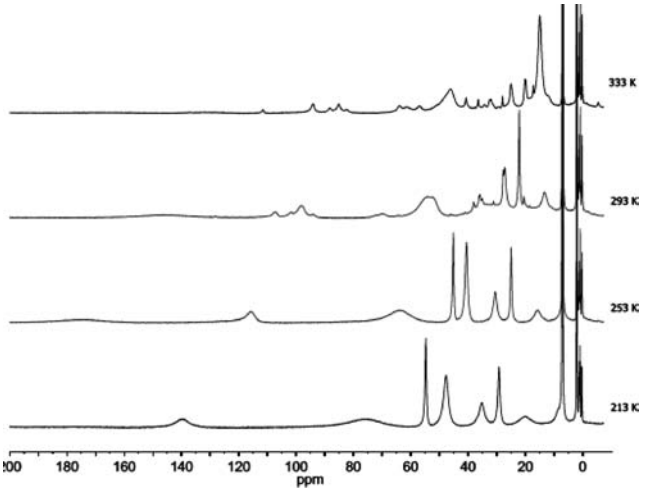

Figure 12. VT ^{1}H NMR spectra of complex [Fe(bapen^F)(Py)$_2$] in d^8-toluene.

assignment of the spectrum was not attempted. At higher temperatures, multiple peaks are observed indicating the presence of other isomers.

Conclusion

In conclusion, we have shown in this study the first syntheses of iron(II) salan and bapen complexes, which can be prepared starting from H_2salan and H_2bapen with [Fe{N(SiMe$_3$)$_2$}$_2$]. Dinuclear complexes of the form [Fe(salan^X)]$_2$] are observed in the solid state and in the presence of suitable donors L, such as pyridine or THF, complexes of the type [Fe(salan^X)(L)$_2$] and [Fe(bapen^X)(L)$_2$] can be isolated. The complexes show a temperature-dependent dynamic behavior in solution, whereby interconversion between the various ligand topologies cis-α, cis-β, and trans occurs. The solid-state structures obtained from X-ray crystallographic analysis of crystals grown from solutions of these complexes only represent one isomer of the mixture present in solution and not necessarily the major isomer. The iron(II) salan and bapen complexes have shown no activity as catalysts for the oxidation of cyclohexane with H_2O_2 as the oxidant under the conditions used here. This lack of catalytic activity is believed to be due to the rapid formation of oxo-bridged iron(III) complexes, which are catalytically inactive. The reaction of iron(II) salan complexes with O_2 has resulted in the isolation of several oxo-bridged Fe(III) complexes, such as [{Fe(salan^{Cl})}$_2$(μ-O)] and [{Fe(salan^H)(Py)}$_2$(μ-O)]. We believe that these oxo-bridged iron(III) complexes are common catalyst degradation products in many homogeneous iron-catalyzed oxidation reactions. The prevention of their formation or their regeneration will be investigated in our future research toward highly active and robust alkane oxidation catalysts.

Acknowledgment. We are grateful to EPSRC and to Unilever for funding and to Johnson Matthey for a generous loan of $RuCl_3$. We thank Peter Haycock and Richard Sheppard for their assistance with NMR measurements.

Supporting Information Available: Crystallographic data and selected bond lengths and angles for complexes [{Fe(salan^{tBu,tBu})}-2(μ-O)] and [Fe(salan^{tBu,tBu})Cl]. Synthetic procedures and analytical data for ligands and metal complexes and VT NMR spectra in d^5-pyridine. This material is available free of charge via the Internet at http://pubs.acs.org.

Note Added after ASAP Publication. This paper was published on the Web on November 9, 2010, with a missing caption for Figure 12. The corrected version was reposted on November 11, 2010.